DEVELOPMENT OF TWO-PHASE FLOW CFD CODE (EAGLE) WITH INTERFACIAL AREA TRANSPORT EQUATION FOR ANALYSIS OF SUBCOOLED BOILING FLOW

B.U. Bae*[1], B.J. Yun[1], H.Y. Yoon[1], G.C. Park[2], C.-H. Song[1]

[1]Thermal Hydraulics Safety Research Division, Korea Atomic Energy Research Institute, Korea
**Phone: +82 (42) 868-2597, Fax: +82 (42) 868-8362, E-Mail: bubae@kaeri.re.kr*
[2]Department of Nuclear Eng., Seoul National University, Korea

Abstract

The interfacial area transport equation for a subcooled boiling flow is developed with a mechanistic model for the wall boiling source term. It includes the bubble lift-off diameter model and the lift-off frequency reduction factor model. Those models take into account a bubble's sliding on the heated wall after a departure from the nucleate site and the coalescences of sliding bubbles. To implement the model, the two-phase flow CFD code was developed, which is named as EAGLE (Elaborated Analysis of Gas-Liquid Evolution). The developed model and EAGLE code are validated by the experimental data of SUBO (Subcooled Boiling) facility. The computational analysis reveals that the interfacial area transport equation with the bubble lift-off diameter model agrees well with the experimental results. It presents that the source term for the wall nucleation enhanced the prediction capability for a multi-dimensional behavior of void fraction or interfacial area concentration.

1. INTRODUCTION

Two-phase flow phenomena with a boiling or condensation are known to be crucial for the nuclear reactor safety. Especially, subcooled boiling phenomenon has become one of the important issues in a design, operation and safety analysis of nuclear power plant. For an example of the phenomena, it can be observed in the downcomer boiling during a Large-Break Loss-of-Coolant Accident (LBLOCA) reflood phase (Song et al., 2007). For the analysis of a subcooled boiling two-phase flow, the two-fluid model is considered as a state-of-the-art model which deals with the mass, momentum and energy of each phase separately. As given in the formulation of the two-fluid model, the interfacial area concentration (IAC), which is defined as the area of an interface per unit mixture volume, is one of the most significant parameters governing the behavior of each phase. In conventional approaches as implemented in the nuclear system analysis codes, IAC models have been developed for a fully developed flow based on a flow regime map. However, due to the static characteristics of those models, it has been reported that they have revealed a weakness in predicting a gradual transition of interfacial structure and induced artificial discontinuities or instabilities during the estimation of interfacial interaction terms (Kelly, 1997).

In order to resolve the problems of the conventional models for IAC, an interfacial area transport equation (IATE) has been developed for an adiabatic bubbly flow or nucleate boiling flow. From the view-point of the boiling source terms, Kocamustafaogullari and Ishii (1983) suggested a basic formulation of the source term in a bubble number density transport equation, which is composed of the bubble departure diameter, the departure frequency, and the nucleate site density. Recently, Yao and Morel (2004) selected some models from the literature for those three parameters and applied them to the analysis of a boiling flow with a one-group interfacial area transport equation. On the other hand, Yeoh and Tu (2005) pointed out a complex mechanism of a bubble on the heated wall, which includes a sliding on the wall after a departure and a lift-off toward the bulk fluid. Situ et al. (2005) set up a force balance on the bubble, so that the bubble lift-off diameter model was developed without considering the bubble departure mechanism. Hence, in order to perform a more realistic two-phase flow analysis for the subcooled boiling, it is required to develop a mechanistic model for the bubble lift-off diameter and implement the model into the source term of the interfacial area transport equation.

For the investigation of the subcooled boiling flow with a dynamic modeling of the interfacial structure, this study aims at the development of an interfacial area transport equation with a

mechanistic model for the bubble lift-off mechanism. To implement the model, a computational fluid dynamics (CFD) code for the two-phase flow analysis is developed, which adopts the two-fluid model and various constitutive models. The developed model and EAGLE code are validated with SUBO (Subcooled Boiling) experiment data for a vertical annulus channel, which was conducted with measuring the local parameters of two-phase flow.

2. MODELING OF INTERFACIAL AREA TRANSPORT EQUATION

2.1. One-group interfacial area transport equation

For a multi-dimensional calculation of the IAC (interfacial area concentration), Yao and Morel (2004) derived an interfacial area transport equation available for a boiling flow as follows.

$$\frac{\partial a_i}{\partial t}+\nabla\cdot\left(a_i V_g\right)=\frac{2}{3}\frac{a_i}{\alpha\rho_g}\left[\Gamma_{ig}-\alpha\frac{d\rho_g}{dt}\right]+\phi_{co}+\phi_{bk}+\phi_{ph} \tag{1}$$

where ϕ_{co} , ϕ_{bk} , and ϕ_{ph} mean the variance of IAC by a coalescence, breakup and nucleation, respectively. The first term on the right-hand side of Eq. (1) is the term of a bubble size variance due to a condensation heat transfer or a pressure drop.

Noting that the subcooled boiling flow in this study is a bubbly flow, the coalescence by a random collision (RC) and the breakup by a turbulent impact (TI) are considered for the second and the third term on the right-hand side of Eq. (1), respectively. Yao and Morel (2004) modeled those terms as follows.

$$\begin{aligned}\phi_{RC}&=-\frac{1}{3\psi}\left(\frac{\alpha}{a_i}\right)^2\cdot\frac{1}{2}\frac{\eta_c n}{T_c}=-\frac{1}{3\psi}\left(\frac{\alpha}{a_i}\right)^2\cdot\frac{1}{2}\frac{\eta_c n}{T_{cf}+T_{ci}}\\&=-\frac{1}{3\psi}\left(\frac{\alpha}{a_i}\right)^2\cdot K_{c1}\frac{\varepsilon^{1/3}\alpha^2}{D_{sm}^{11/3}}\cdot\frac{1}{g(\alpha)+K_{c2}\alpha\sqrt{We/We_c}}\cdot\exp\left(-K_{c3}\sqrt{\frac{We}{We_c}}\right)\end{aligned} \tag{2}$$

$$\begin{aligned}\phi_{TI}&=\frac{1}{3\psi}\left(\frac{\alpha}{a_i}\right)^2\cdot\frac{\eta_b n}{T_b}=\frac{1}{3\psi}\left(\frac{\alpha}{a_i}\right)^2\cdot\frac{\eta_b n}{T_{bf}+T_{bi}}\\&=\frac{1}{3\psi}\left(\frac{\alpha}{a_i}\right)^2\cdot K_{b1}\frac{\varepsilon^{1/3}\alpha(1-\alpha)}{D_{sm}^{11/3}}\cdot\frac{1}{1+K_{c2}(1-\alpha)\sqrt{We/We_c}}\cdot\exp\left(-\frac{We}{We_c}\right)\end{aligned} \tag{3}$$

where ψ is a bubble shape factor, 1/36π for a spherical bubble, and η and n are the interaction efficiency of neighboring bubbles and the bubble number density, respectively. *We* is a Weber number and ε is the dissipation, which can be obtained from the k-ε model. $g(\alpha)$ is a modification factor defined as $1-(\alpha/\alpha_{\max})^{1/3}$, and the coefficients in the equations are K_{c1}=2.86, K_{c2}=1.922, K_{c3}=1.017, We_c=1.24, $\alpha_{\max}$=0.52, K_{b1}=1.6, K_{b2}=0.42.

The last term on the right-hand side in Eq. (1) denotes an increase of IAC by a bubble nucleation at the heated wall, that is, the boiling source term in the interfacial area transport equation. It is composed of a product of the active nucleate site density (*N''*), the bubble departure diameter (D_d) and the bubble departure frequency (*f*), as presented in Eq. (4).

$$\phi_{ph}=\pi D_d^2\cdot\frac{N''\cdot f\cdot A_H}{\mathrm{Vol}} \tag{4}$$

, where A_H is the area of heated surface and Vol is the volume of a control volume.

In previous studies, the boiling source term of interfacial area transport equation had been modeled according to a bubble departure mechanism as shown in Eq. (4). That is, it estimates the evaporation induced by the departure of a bubble at the heated wall. In that modeling, the bubble generated at a nucleate site is assumed to depart from the wall with the bubble departure frequency. However, it was

observed that the actual behavior of the bubbles at the wall was more complex than the departure mechanism. The bubble departing from a nucleate site slides along the wall without directly moving to the bulk liquid as depicted in Fig. 1. During the sliding, the bubble size can be varied by the superheated liquid layer on the wall, so that the bubble diameter at the lift-off is different with the bubble departure diameter. Moreover, when a sliding bubble encounters another departing bubble at a nucleation site, a coalescence between two bubbles occurs and the bubble size is enlarged. Therefore, in this study, a modified form of the boiling source term is discussed in the following sections by considering the lift-off diameter and the reduction factor for the lift-off frequency.

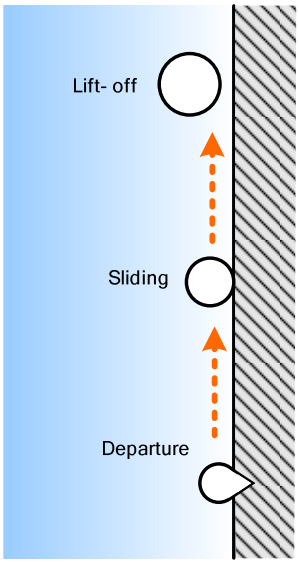

Fig. 1 Mechanism of sliding and lift-off of the bubble

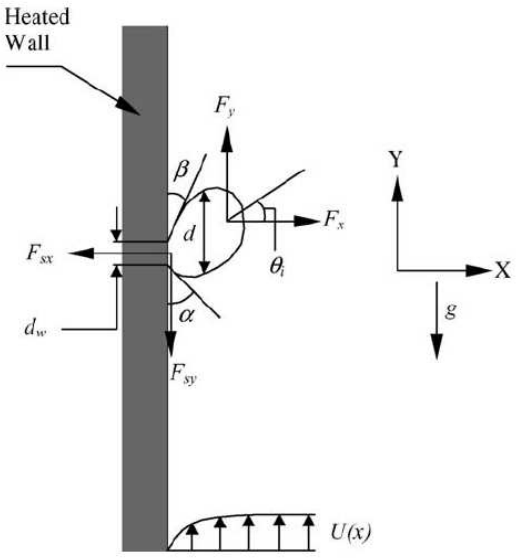

Fig.2 Force balance on a bubble at the wall (Yeoh, 2005)

2.2. Modeling of bubble lift-off diameter

To determine the bubble size at a lift-off from the heated wall, a force balance on a sliding bubble along the wall should be considered. Yeoh and Tu (2005) investigated the force balance on a bubble from the studies of Klausner et al. (1993) and Zeng et al. (1993), which is presented in Fig. 2. At the moment of a bubble lift-off, the force balance on the bubble in the x-direction is violated and the contact diameter at the wall becomes zero. Therefore, the force balance on the lifting bubble of radius r is given as follows.

$$-\rho_f \pi r^2 \left(\frac{3}{2} C_s r'^2 + r \cdot r'' \right) \cos\theta_i + \frac{1}{2} C_{sl} \rho_f \pi r^2 u_r^2 = 0 \qquad (5)$$

where the first term on the left-hand side is an unsteady drag force and the second term is a shear lift force. θ_i is the bubble inclination angle and u_r is the relative velocity between the bubble and liquid. C_{sl}, the shear lift force coefficient, has been modeled by Klausner et al. (1993). The coefficient C_s is given as 20/3 according to Zeng's study (1993), then Eq. (5) is reduced to Eq. (6).

$$10 r'^2 + r \cdot r'' = \frac{1}{2\cos\theta_i} C_{sl} u_r^2 \qquad (6)$$

To resolve Eq. (6), the function for a bubble growth with respect to time is required. Zuber (1961) derived it by considering a thermal diffusion in the superheated liquid.

$$\rho_g h_{fg} \frac{dr}{dt} = \frac{k\left(T_w - T_{sat}\right)}{\sqrt{\pi \eta t}} \qquad (7)$$

where η is a thermal diffusivity of liquid. Regarding that the bubble departure occurs at t=0, the bubble growth function can be derived with integrating Eq. (7) from t=0, as follows.

$$r(t) = r_d + \frac{2b}{\sqrt{\pi}} Ja\sqrt{\eta t} \tag{8}$$

where r_d is the bubble radius at the departure from the wall and *Ja* is the Jacob number.

In the other hand, the bubble radius at the moment of a lift-off, r_{lo}, can be related with the lift-off time, t_{lo}, as $r_{lo} = r_d + A\sqrt{t_{lo}}$. Then substituting Eq. (8) into Eq. (6), a relation for the lift-off time is found as,

$$9A^2 t_{lo}^{-1} - Ar_d t_{lo}^{-\frac{3}{2}} = \frac{2}{\cos\theta_i} C_{sl} u_r^2 \quad \text{where } A = \frac{2b}{\sqrt{\pi}} Ja\sqrt{\eta} \tag{9}$$

Then Eq. (9) can be formulated with respect to the bubble growth ratio, r^*.

$$\frac{9}{r^{*2}} - \frac{1}{r^{*3}} = \frac{2}{\cos\theta_i} C_{sl} \left(\frac{r_d u_r}{A^2} \right)^2 \quad \text{where} \quad r^* \equiv \frac{r_{lo} - r_d}{r_d} \tag{10}$$

Hence, the explicit formulation for the bubble lift-off diameter (D_{lo}) is derived as,

$$D_{lo} = D_d \left(1 + r^*\right) = D_d \left(1 + 8.34 \left[\frac{C_{sl}}{\cos\theta_i} \cdot \left(\frac{D_d u_r}{A^2} \right)^2 \right]^{-0.7} \right) \tag{11}$$

where Unal's model (1976) is adopted for the departure diameter (D_d).

2.3. Modeling of lift-off frequency reduction factor

During the sliding of a departed bubble, coalescences can occur with another bubble at a nucleate site. It reduces the number of actual bubble lift-offs from the wall, with respect to the nucleate site density for the bubble departure, so that it affects a nucleation source term in the interfacial area transport equation. Therefore lift-off frequency reduction factors are considered for the boiling source term in the interfacial area transport equation as follows.

$$\phi_{ph} = \pi D_{lo}^2 \cdot R_a N'' f \cdot \frac{A_H}{Vol} \tag{12}$$

where R_a is a reduction factor for the interfacial area concentration.

In order to model the lift-off frequency reduction factors, a sliding length and a spacing of the nucleate site should be considered. The sliding length, l_0, is a distance from the departure to the lift-off of a bubble on the wall, assuming that the departed bubble does not encounter any coalescence during the sliding. The spacing, s, is an average distance between two neighboring nucleate sites. When the spacing is shorter than the bubble departure diameter, D_d, the bubble at a nucleation site cannot grow until the size reaches the bubble departure diameter and it lifts off the wall with the diameter of s without a sliding. Hence, the reduction factors are determined as follows.

$$R_a = \left(s / D_{lo}\right)^2 \text{ for } s < D_d \tag{13}$$

When l_0 is shorter than the spacing, there is no coalescence among the departed bubbles on the wall and all bubbles lift off the wall with a diameter of D_{lo} as defined in Eq. (11). It suggests that the reduction factors become unity, that is,

$$R_a = 1 \text{ for } l_0 < s \tag{14}$$

When the spacing is longer than the departure diameter (D_d) and shorter than l_0, the bubble generated at a nucleation site can begin sliding and form coalescences with other bubbles during the sliding. In this region, the lift-off frequency reduction factor is assumed to be a linear function between the no-sliding region (Eq. (13)) and no-coalescence region (Eq. (14)), so those are estimated as follows.

$$R_a = \left(1 - \frac{D_d^2}{D_{lo}^2}\right)\left(\frac{s - D_d}{l_0 - D_d}\right) + \frac{D_d^2}{D_{lo}^2} \text{ for } D_d < s < l_0 \tag{15}$$

3. CODE STRUCTURE

3.1 Governing equations

To implement the interfacial area transport equation discussed in Section 2, the computational fluid dynamics (CFD) code, EAGLE (Elaborated Analysis of Gas-Liquid Evolution), is developed in this study. The code aims at the multi-dimensional analysis of subcooled boiling two-phase flow, by utilizing the dynamic approach of the interfacial area transport equation.

EAGLE code adopts the two-fluid model, which is beneficial to treat the behavior of each phase separately and to consider a phase interaction term properly. As derived in the two-fluid model by Ishii (1984), the mass balance equation for a phase is given as,

$$\frac{\partial\left(\alpha_k \rho_k\right)}{\partial t} + \nabla \cdot \left(\alpha_k \rho_k \mathbf{u}_k\right) = \Gamma_k \tag{16}$$

where Γ_k is the rate of a phase change for the k phase.

The momentum equations are given as follows.

$$\begin{aligned}\frac{\partial\left(\alpha_k \rho_k u_k\right)}{\partial t} + \nabla \cdot \left(\alpha_k \rho_k \mathbf{u}_k u_k\right) = &-\nabla\left(\alpha_k p\right) + \nabla \cdot \left[\alpha_k \left(\overline{\overline{\tau}}_k + \tau_k^T\right)\right] + \alpha_k \rho_k \mathbf{g} \\ &+ u_{ki}\Gamma_k + F_{ik} - \nabla \alpha_k \cdot \tau_{ki} + p \nabla \alpha_k\end{aligned} \tag{17}$$

where $\overline{\overline{\tau}}_k$ and τ_k^T are the molecular stress tensor and the turbulent stress tensor, respectively. F_{ik} denotes the term of an interfacial momentum transfer including the interfacial drag force, the wall lubrication force, the lift force, the turbulent dispersion force and the virtual mass force (Ishii and Hibiki, 2006). The details of each force was omitted in this paper due to the limitation of pages and the sensitivity test on each force in EAGLE code has been performed in the authors' previous paper. (Bae, 2008)

Energy equations are expressed as a form of the enthalpy $\left(H_k\right)$ transport of each phase.

$$\frac{\partial\left(\alpha_k \rho_k H_k\right)}{\partial t} + \nabla \cdot \left(\alpha_k \rho_k H_k \mathbf{u}_k\right) = -\nabla \cdot \left[\alpha_k \left(\overline{\overline{\mathbf{q}}}_k + \mathbf{q}_k^T\right)\right] + \alpha_k \frac{D_k p}{Dt} + H_{ki}\Gamma_k + q_{ki}^{''} a_i + \Phi_k \tag{18}$$

where $\mathbf{q}_k$ is a diffusive flux by a conduction and the superscript 'T' means the enhanced flux by a turbulence. $q_{ki}^{''}$ is the interfacial heat flux between two phases, defined as $h_i\left(T_s - T_k\right)$, and a_i is the interfacial area concentration. Φ_k is an external source term for a phase.

A semi-implicit method is usually used for transient problems of the fluid dynamics, where an implicit method struggles with a convergence of the solution. Two-phase flow phenomena have transient characteristics in most cases, so that the semi-implicit method can be applied effectively. Among the various semi-implicit methods, the Simplified Marker And Cell (SMAC) algorithm (Amsden et al., 1971), which was originally developed for a single-phase flow, is known to be advantageous for avoiding repeated iterations. For an application of the algorithm to the subcooled boiling flow in this study, the original SMAC algorithm has been extended to a two phase flow with a phase change. (Bae et al., 2008)

3.2 Turbulence model in the two-phase flow

Liquid turbulence is estimated by the standard *k-ε* model, which is a kind of Reynolds-Averaged Navier-Stokes (RANS) equation. For the case of bubbly two-phase flow, the effect of a bubble's motion on the turbulence has been modeled as a term of the bubble diameter and relative velocity (Lahey, 2005). Then, the total turbulent viscosity of the liquid phase is defined as Eq. (19).

$$\mu_t = C_\mu \frac{k_f^2}{\varepsilon_f} + 0.6 D_{sm} \alpha_g \left|v_r\right| \tag{19}$$

In the case of a boiling flow, boiling bubbles at a heated surface are known to considerably affect the turbulence structure near the wall by altering the velocity field in a laminar sublayer. Kataoka and

Serizawa (1997) modeled the enhanced turbulence by boiling bubbles and modified the turbulence mixing length in the boiling region.

$$l_{TP}^{boil} = l_{TP}\left(1+\frac{6q_{ev}}{\rho_g h_{fg}\alpha_p u_l^{'}}\right) \quad (20)$$

q_{ev} in Eq. (20) is the evaporative heat flux. α_p is the void fraction at $y = D_d/2$ and $u_l^{'}$ means the fluctuation, $\sqrt{k}$. In the definition of turbulence mixing length model, turbulent viscosity is proportional to the turbulence mixing length, that is, $\mu_t = \rho_l l_{TP} u_l^{'}$. Therefore, the increased turbulence near the heated surface and wall shear stress were modeled with a same multiplication factor of Eq. (20).

$$\mu_t^{boil} = \mu_t\left(1+\frac{6q_{ev}}{\rho_g h_{fg}\alpha_p u_l^{'}}\right),\ \tau_w^{boil} = \tau_w\left(1+\frac{6q_{ev}}{\rho_g h_{fg}\alpha_p u_l^{'}}\right) \quad (21)$$

Moreover, Kataoka and Serizawa (1997) derived a source term for the turbulent kinetic energy induced by the boiling bubbles, as revealed in Eq. (22)

$$\Phi = \frac{8}{9}\cdot\frac{g\Delta\rho}{\rho_l}\cdot\frac{q_{ev}}{\rho_g h_{fg}} \quad (22)$$

To mechanistically model the turbulence structure, the source term defined in Eq. (22) was additionally considered as a source term of the *k*-transport equation.

4. ANALYSIS RESULTS

4.1 SUBO Experiment

To validate the EAGLE code with the bubble lift-off model, the experimental data of SUBO tests were utilized (Yun et al., 2008a and 2008b). In the experiment, the subcooled boiling phenomena in a vertical annulus channel were observed in SUBO (Subcooled Boiling) facility as shown in Fig. 3. The inner diameter of the test section is 35.5mm and the outer diameter of the heater rod is 10.02mm. The heater rod consists of three parts. The first part is an unheated section with 222mm in length for regulating the water condition at the inlet, the second part is a heated section with 3098mm in length for the simulation of boiling, and the third part is an unheated section with 800mm in length for the bubble condensation at the top region. Local two-phase flow parameters such as a void fraction, interfacial area concentration, bubble velocity were measured by an optical fiber two-sensor probe, which are traversed through 12 positions in a radial direction at 6 levels.

The test conditions of SUBO experiments are summarized in Table 1. Compared with other facilities in the literature, SUBO has a capacity for simulating experimental conditions of the higher heat flux and mass flux in a longer vertical channel. Outlet pressure was maintained at around 155kPa in all the cases. When compared to the Base case, the Q1 and Q2 cases are tested to investigate the effect of heat flux. Moreover, in order to observe the subcooled boiling phenomena according to various conditions, the V1 and V2 cases have a higher mass flux than the base case and the T1 case has a higher inlet subcooling condition.

Table 1 Test matrix of SUBO experiment

Case	Heat flux (kW/m^2)	Mass flux (kg/m^2s)	Inlet subcooling (K)	Inlet pressure (kPa)	Outlet pressure (kPa)
Base	470.6	1132.6	19.1	192.9	157.3
Q1	363.7	1119.6	19.0	192.7	156.7
Q2	563.0	1126.9	18.3	188.9	155.7
V1	465.7	2126.5	19.6	196.9	156.9
V2	567.9	2128.8	19.5	197.6	158.0
T1	465.5	1103.9	29.6	190.7	155.0

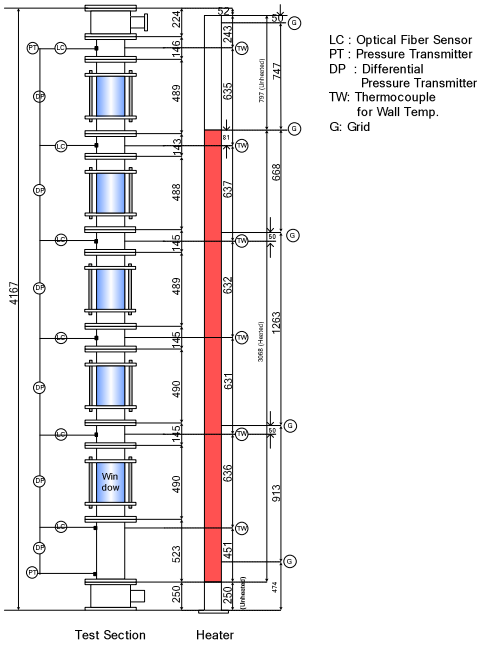

Fig. 3 Test section of SUBO facility

4.2 Result and discussion

To validate EAGLE code and the interfacial area transport equation model in this study, SUBO experiment data was analyzed. Analysis was conducted for modeling the heated section within a grid composed of 10 (radial) x 200 (axial) axisymmetric cells in a cylindrical coordinate. The inlet turbulence intensity was set to 5% of the mean velocity. The grid in the EAGLE analysis was constructed with referring those of previous studies for similar subcooled boiling flow channels. In the CFX analysis of Yeoh and Tu (2005), the grid of 13 (radial)□30 (axial) x 3 (circumference) cells was used for an annulus channel with a 9.25mm gap size and Yao and Morel (2004) used the grid of 13 (radial)□30 (axial) cells for an annulus of 9.6mm gap in NEPTUNE code. In this study, the comparison with a more refined grid was conducted additionally, so that the results between 10 cells and 15 cells in a radial direction will be discussed. The inlet condition and the heated wall boundary condition were given as a constant mass flux and heat flux at the cell surface, and a zero-gradient condition was taken into account at the outlet boundary.

Fig. 4 compares the radial distribution of the void fraction for all test cases of SUBO experiment, respectively. As shown in the figure, the radial distribution of void fraction indicated the existence of bubbly boundary layer near the heated surface, which is one of the representative characteristics in the subcooled boiling phenomena as reported by Lee et al. (2002) and Situ et al. (2004). The thickness of the bubbly boundary layer can be found with the distance from the heater surface to the radial position where the void fraction is zero. It was shown that the bubbly boundary layer was increasing as the fluid flowed toward the downstream within the heated section. In the case of the analysis results as shown in Fig. 3, the axial development of the bubbly boundary layer in the subcooled boiling was predicted reasonably by the calculation of EAGLE code. It means that the evaporative heat flux in the heat partition model according to the bubble lift-off mechanism could estimate the amount of void generation at a heated wall appropriately. The difference of the bubbly boundary layer thickness between the experiment and analysis was due to the limitation of the interfacial heat transfer model, which should be improved depending on the local two-phase flow parameters.

In the comparison of the interfacial area concentration as revealed in Fig. 5, it was found that the modeling of the interfacial area transport equation predicted the distribution of the interfacial area in SUBO experiments appropriately. As revealed in the experimental results, the amount of interfacial area concentration was closely related to the void fraction and the dependency on the heat flux or mass flux condition could be explained by the same reason discussed in the above section. Calculation

results showed that the advanced source term of interfacial area transport equation according to the bubble lift-off mechanism induced a peak of the interfacial area concentration near the heated wall, while the condensation and bubble interaction mechanism such as a breakup or a coalescence predicted the radial distribution of the interfacial area concentration effectively. Fig. 6 compares the interfacial area concentration in Base case with the calculation results adopting Situ's bubble lift-off diameter model (2005). From the comparison, it is proved that the bubble lift-off model derived in Section 2 yields a more reasonable agreement in the multi-dimensional distribution of interfacial area concentration near the heated wall, since the model considers the growth of a departed bubble on the wall mechanistically.

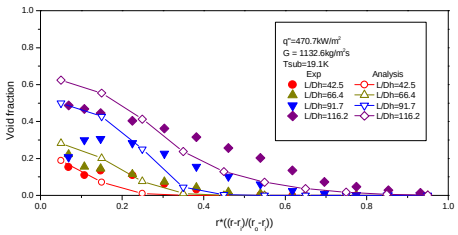

(a) Base case

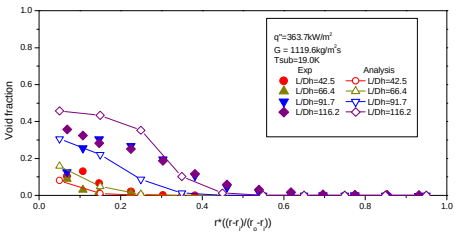

(b) Q1 case

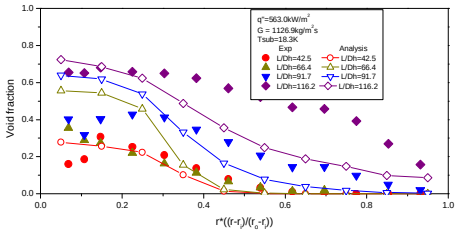

(c) Q2 case

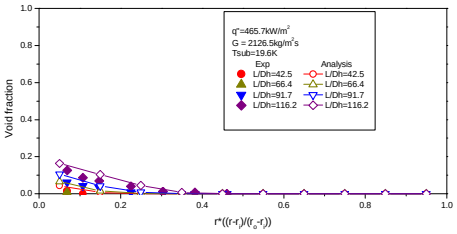

(d) V1 case

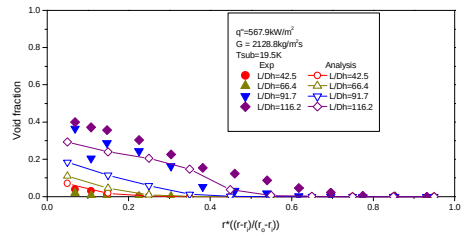

(e) V2 case

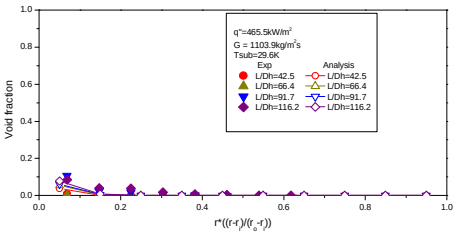

(f) T1 case

Fig. 4 Comparison of void fraction in SUBO experiment

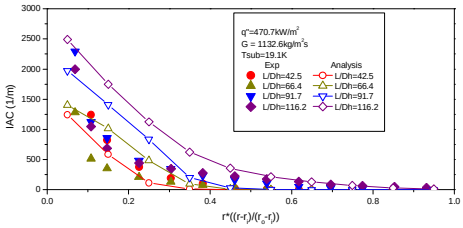

(a) Base case

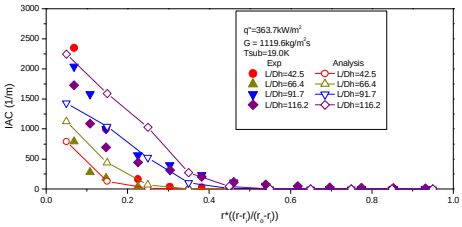

(b) Q1 case

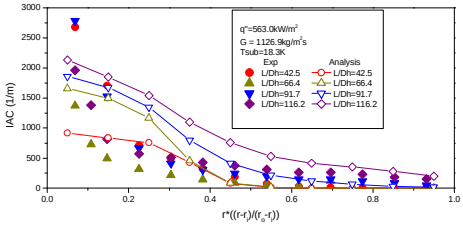

(c) Q2 case

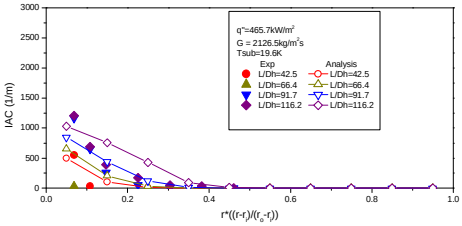

(d) V1 case

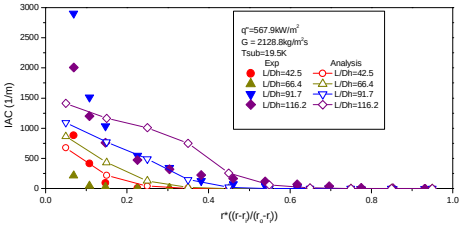

(e) V2 case

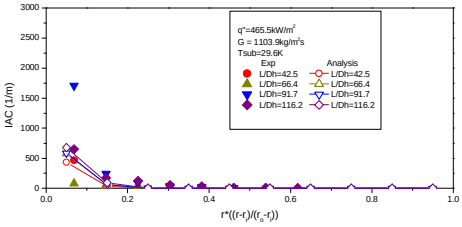

(f) T1 case

Fig. 5 Comparison of interfacial area concentration in SUBO experiment

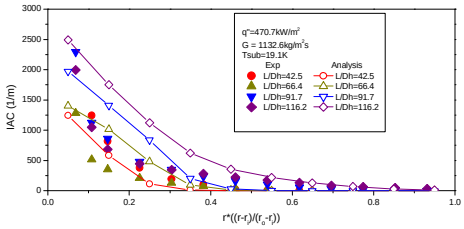

(a) Bubble lift-off model in this study

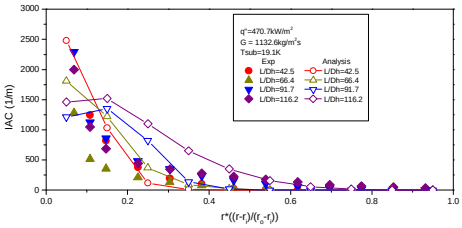

(b) Situ's lift-off diameter model (2005)

Fig. 6 Comparison of interfacial area concentration in Base case

Fig. 7 represents the analysis results of the bubble velocity and compares them with the experimental ones. As seen in the experimental results, the axial bubble velocity showed a peak at around the center of the channel due to a larger buoyant force of the large bubbles. EAGLE code analysis also revealed a peak of bubble velocity at around the center in all test cases and indicated a reasonable agreement with the experimental results as shown in the figure. Especially, the modeling of an increased turbulence in the laminar sublayer as described in Section 3.2 played an important role in enhancing the prediction capability of the bubble velocity near the heated surface. The modeling effect is compared in Fig. 8, where the calculation with excluding the enhanced turbulence overestimated the bubble velocity near the heated wall. The wall function according to the single phase flow turbulence was applied to calculate the wall shear stress, which is equal to a diffusive flux term acting on the surface of a cell adjacent to the wall. The shape of velocity profile as depicted in EAGLE analysis results could be parabolic by the effect of the wall shear stress. The assumption of velocity profile according to the wall function theory can be available only in a region which is closely adjacent to the wall. So the parabolic shape of the velocity in Fig. 8 is not directly related with the velocity profile according to the wall function itself.

On the other hand, the bubble velocity in the downstream is not significantly increased due to the momentum balance between the interfacial frication and buoyancy force. As compared to the Base, Q1, and Q2 cases in Fig. 7, the high heat flux generated a larger amount of steam in both of experiment and analysis and it caused the bubble velocity increased. In the V1 and V2 cases with the larger mass flux, although the void generation was less than the Base or Q2 cases due to the higher subcooling of the fluid, bubble velocity was increased by the interaction with the liquid phase.

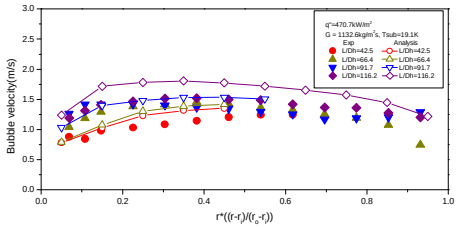

(a) Base case

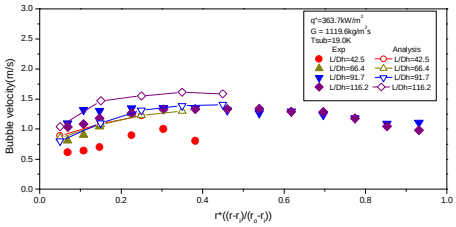

(b) Q1 case

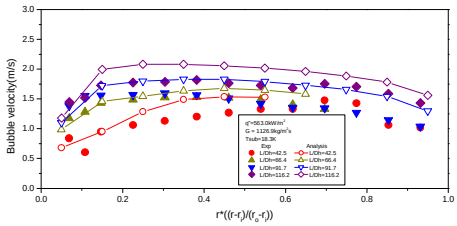

(c) Q2 case

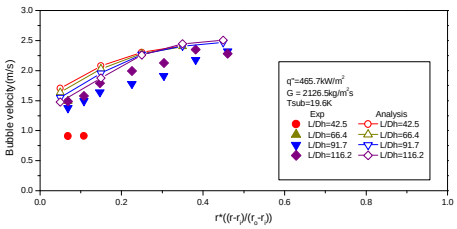

(d) V1 case

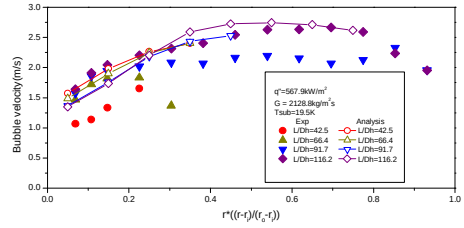

(e) V2 case

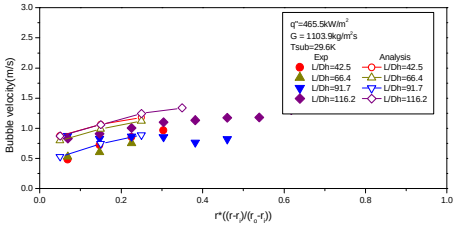

(f) T1 case

Fig. 7 Comparison of bubble velocity in SUBO experiment

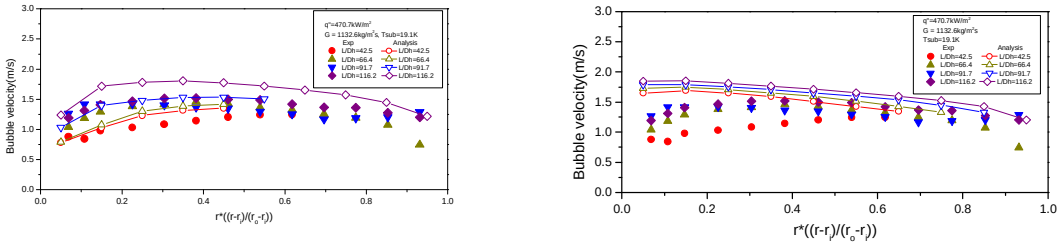

(a) With the turbulence of boiling bubbles (b) Without the turbulence of boiling bubbles

Fig. 8 Comparison of bubble velocity in Base case

Fig. 9 compares the analysis results of Base case with a more refined grid. (15 radial cells x 200 axial cells) As shown in the figure, the more refined grid in a radial direction did not significantly influence the analysis results.

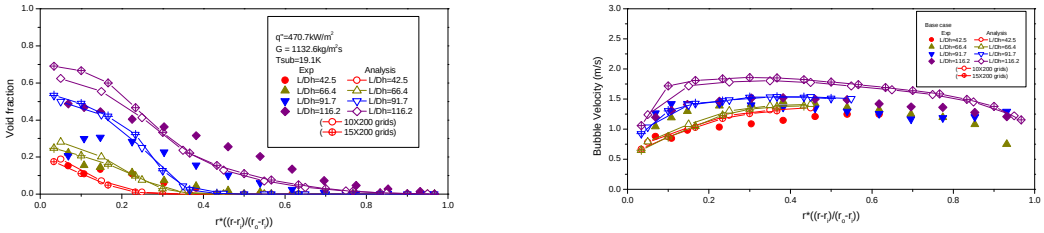

(a) Void fraction (b) Bubble velocity

Fig. 9 Effect of grid refinement in Base case

5. CONCLUSION

This study focused on the development of a wall nucleation source term for the interfacial area transport equation for the analysis of the subcooled boiling two-phase flow. To evaluate the model, SUBO experiment was performed and the test results were utilized for the validation of EAGLE code. To mechanistically model the dynamic behavior of the interfacial area concentration, the wall nucleation source term in the interfacial area transport equation was improved with taking into account the bubble sliding and lift-off phenomena on the wall. Bubble lift-off diameter model was developed from a force balance on the sliding bubble at the heated wall. In order to consider the actual frequency of the bubble lift-off, the effect of a coalescence among the sliding bubbles was reflected by modeling the lift-off frequency reduction factor, which affected the evaporative heat flux and the wall nucleation source term in the interfacial area transport equation. The interfacial area transport equation with the developed wall nucleation model has been implemented in the multi-dimensional two-phase flow analysis code, EAGLE. The code adopted the two-fluid model and SMAC algorithm was extended to be applicable to the two-phase flow with a phase change.

From a comparison with SUBO experiment, the analysis with a mechanistic model of bubble lift-off diameter and lift-off frequency reduction factor was confirmed to predict the experimental data reasonably well. In conclusion, the development of EAGLE code with the mechanistic model of the interfacial area transport equation will enhance the analysis capability of multi-dimensional two-phase flow during the subcooled boiling. As a further improvement following this work, development of the

two-group interfacial area transport equation for a boiling flow is essential to cover the flow regime of a bubbly-to-slug transition flow or a slug flow.

REFERENCES

Amsden, A. A. *et al.*, *The SMAC Method : A numerical technique for calculating incompressible fluid flow*, Report LA-4370, Los Alamos Scientific Lab. (1971).

Bae, B. U., Yoon, H. Y., Euh, D. J., Song, C-. H., Park, G. C., "Computational Analysis of a Subcooled Boiling Flow with a One-group Interfacial Area Transport Equation", *Journal of Nuclear Science and Technology*, **45[4]**, 341-351 (2008).

Euh, D.J., Yun, B.J, Song, C-.H., "Investigation of the Transport of the Bubble Parameters in Air/Water Flow Conditions", *ICAPP05*, Seoul, Korea (2005).

Kataoka, I., Serizawa, A., "Analysis of turbulence structure of gas-liquid two-phase flow under forced convective subcooled boiling", *Proc. 2nd Japanese-German Symposium on Multi-phase Flow*, Tokyo, Japan (1997).

Kelly, J., "Constitutive model development needs for reactor safety thermal-hydraulic code," *Proceedings of the OECD/CSNI Specialist Meeting on Advanced Instrumentation and Measurement Techniques*, Santa Barbara, U.S. (1997).

Klausner, J. F., Mei, R., Bernhard, D.M., Zeng, L.Z., "Vapor bubble departure in forced convective boiling", *Int. J. Heat Mass Transfer*, **36**, 651-662 (1993).

Kocamustafaogullari, G., Ishii, M., "Interfacial area and nucleate site density in boiling systems", *Int. J. Heat Mass Transfer*, **26[9]**, 1377-1387 (1983).

Lahey Jr., R. T., "The simulation of multidimensional multiphase flows", *Nuclear Engineering and Design*, **235**, 1043-1060 (2005).

Lee, T. H., Park, G. C., Lee, D. J., "Local flow characteristics of subcooled boiling flow of water in a vertical concentric annulus", *Int. J. Multiphase Flow*, 2**8**, 1351-1368 (2002).

Situ, R., Hibiki, T., Ishii, M., Mori, M., "Bubble lift-off size in forced convective subcooled boiling flow", *Int. J. Heat Mass Transfer*, **48**, 5536-5548 (2005).

Situ, R., Hibiki, T., Sun, X., Mi, Y., Ishii, M., "Flow structure of subcooled boiling in an internally heated annulus", *Int. J. Heat Mass Transfer*, **47**, 5351-5364 (2004).

Song, C-. H., Baek, W. P., Park, J. K., "Thermal-hydraulic test and analyses for the APR1400's development and licensing", *Nuclear Engineering and Technology*, 39[4], 299-312 (2007).

Unal, H. C., "Maximum bubble diameter, maximum bubble growth time and bubble growth rate during the subcooled nucleate flow boiling of water up to 17.7MN/m^2," *Int. J. Heat Mass Transfer*, **19**, 643-649 (1976).

Yao, W., Morel, C., "Volumetric interfacial area prediction in upward bubbly two-phase flow," *Int. J. Heat and Mass Transfer*, **47**, 307-328 (2004).

Yeoh, G. H., Tu, J. Y., "A unified model considering force balances for departing vapour bubbles and population balance in subcooled boiling flow," *Nuclear Engineering and Design*, **235**, 1251-1265 (2005).

Yun, B.J., Bae, B.U., Park, W.M., Euh, D.J., Song, C.H., "Experimental study of local bubble parameters of the subcooled boiling flow in a vertical annulus channel", KAERI/TR-3562/2008 (2008a).

Yun, B.J., Bae, B.U., Park, W.M., Euh, D.J., Song, C.H., "Characteristics of local bubble parameters of subcooled boiling flow in an annulus", Experiments and CFD Code Applications to Nuclear Reactor Safety, OECD/NEA Workshop, Grenoble, France, 10-12 September (2008b).

Zeng, L. Z., Klausner, J. F., Bernhard, D.M., Mei, R., "A unified model for the prediction of bubble detachment diameters in boiling systems. II. Flow boiling", *Int. J. Heat Mass Transfer*, **36**, 2271-2279 (1993).

Zuber, N., "The dynamics of vapor bubbles in nonuniform temperature fields", *Int. J. Heat Mass Transfer*, **2**, 83-98 (1961).